Observations of reconnection exhausts associated with large-scale current sheets within a complex ICME at 1 AU

X. Xu,[1,2] F. Wei,[1] and X. Feng[1]

Received 29 September 2010; revised 13 February 2011; accepted 24 February 2011; published 28 May 2011.

[1] During 26–27 November 2000 a complex interplanetary coronal mass ejection, composed of four flux ropes, was detected by Wind and ACE at 1 AU. We identify two Petschek-like exhaust events within the interiors of the second and third flux ropes, respectively. In the first event, Wind and ACE detected an exhaust at the same side from the reconnection site, which was associated with a large-scale bifurcated current sheet with a spatial width of ~10,000 ion inertial lengths and the magnetic shear was 155°. In the second event, the two spacecraft observed the oppositely directed exhausts from a single reconnection X line. The exhausts were also related to a large-scale current sheet with a spatial width of ~3000 ion inertial lengths and a shear angle of about 135°. The two exhaust events resulted from fast and quasi-stationary reconnection. The related current sheets were both flat on the scale of a few hundred Earth radii and located close to the centers of subflux ropes. The decrease of radial expansion speed of each flux rope might account for the formation of the two current sheets. Reconnections at the centers of flux ropes may change the entire topology of the flux ropes and may fragment them into smaller ones.

Citation: Xu, X., F. Wei, and X. Feng (2011), Observations of reconnection exhausts associated with large-scale current sheets within a complex ICME at 1 AU, *J. Geophys. Res.*, *116*, A05105, doi:10.1029/2010JA016159.

1. Introduction

[2] Magnetic reconnection is a universal plasma dissipation process which converts magnetic energy into particle energy and changes the magnetic field topology. Reconnection at the magnetopause and magnetotail plays an important role in the Earth space weather system, and has been confirmed by many direct in situ observations [e.g., *Mozer et al.*, 2002; *Vaivads et al.*, 2004; *Øieroset et al.*, 2001].

[3] Recently, many reconnection observations in the solar wind were reported [e.g., *Gosling et al.*, 2005b; *Davis et al.*, 2006; *Phan et al.*, 2006]. A large number of these reconnection events have been found to be associated with interplanetary coronal mass ejections (ICMEs). These ICME-related reconnection reports together with simulation results in the solar wind can be classified into three types based on the occurrence locations: (1) between ICMEs and ambient solar wind [*Schmidt and Cargill*, 2003; *Gosling et al.*, 2007b; *Gosling and Szabo*, 2008]; (2) between ICME and ICME [*Lugaz et al.*, 2005]; (3) within the interior of ICMEs [*Gosling et al.*, 2007b; *Gosling and Szabo*, 2008].

[4] ICMEs, the interplanetary manifestations of CMEs, have two subsets according to the magnetic field signatures, i.e., magnetic clouds (MCs), characterized by their high magnetic field magnitude, the rotation of the magnetic field direction and low proton temperature [*Burlaga et al.*, 1981], and non-MC-like ICMEs. Some complex non-MC-like ICMEs could be conglomerates of several individual ICMEs [*Zurbuchen and Richardson*, 2006] or consist of several flux tubes [*Fainberg et al.*, 1996]. A complex ICME consisting of several substructures could contain all the three types of these ICME-associated reconnection events mentioned above. Therefore, reconnection in this area may have a good possibility to occur and to be detected.

[5] *Gosling et al.* [2005b] showed the direct evidence for identification of Petschek-like magnetic reconnection [*Petschek*, 1964] exhausts in the solar wind, i.e., jetting plasma emanating from reconnection sites and bounded by pairs of back-to-back rotational discontinuities, or observationally, a pair of correlated (anticorrelated) and anticorrelated (correlated) variations in **B** and **V** at the edges of the exhaust. Using the direct evidence, many X line exhausts were reported [e.g., *Gosling*, 2007, *Gosling et al.*, 2007a, 2007b]. In most multispacecraft observations of reconnection exhausts, the different spacecraft detect only one of the predicted pair of exhausts from a given reconnection X line [*Phan et al.*, 2009]. However, *Davis et al.* [2006] and *Gosling et al.* [2007a] have reported multispacecraft observations of the oppositely directed jets from X lines. In this paper, we report two in situ dual spacecraft detections of Petschek-like exhaust events, including an oppositely

[1]SIGMA Weather Group, State Key Laboratory of Space Weather, Center for Space Science and Applied Research, Chinese Academy of Sciences, Beijing, China.
[2]College of Earth Sciences, Graduate University of Chinese Academy of Sciences, Beijing, China.

0148-0227/11/2010JA016159

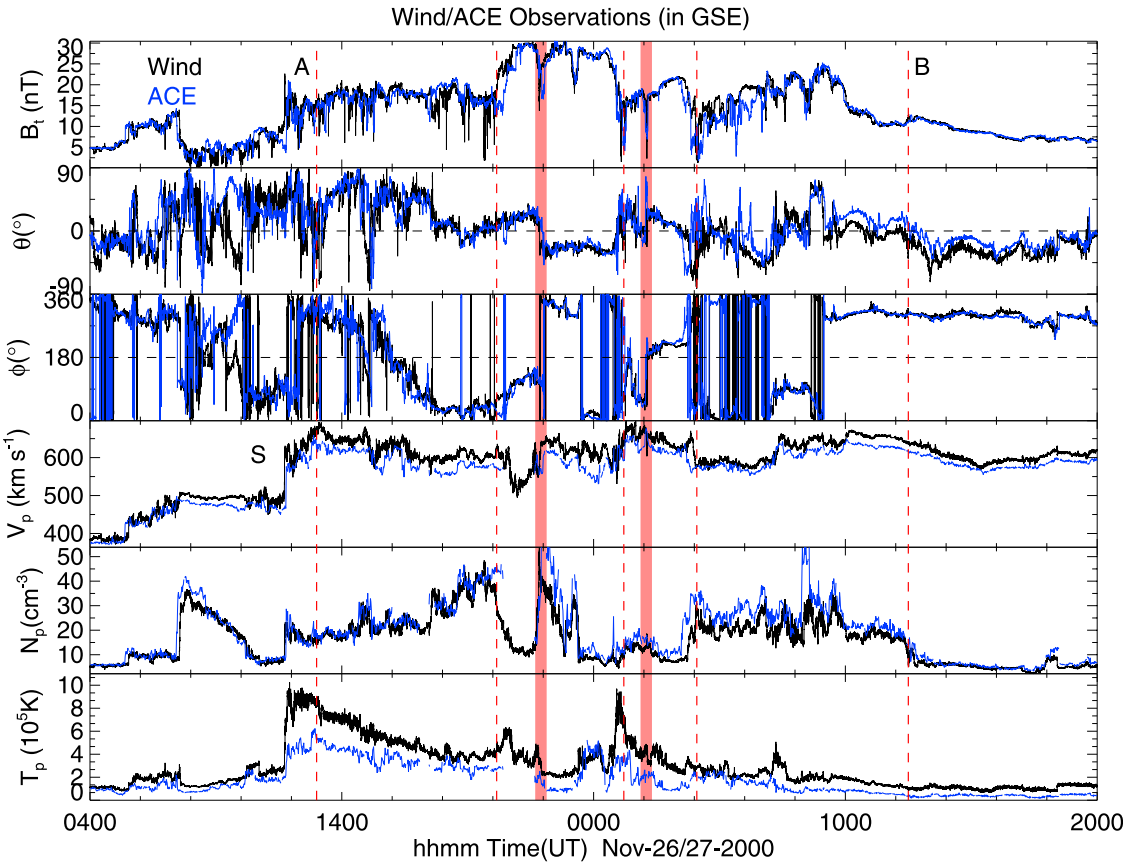

Figure 1. Observations by Wind and ACE in GSE from 26 November (0400 UT) to 27 November (2000 UT) 2000. (top to bottom) Magnetic field strength $\mathbf{B_t}$, magnetic latitude θ, magnetic azimuth ϕ, proton speed V_p, proton density N_p, and proton temperature T_p. Vertical dashed lines denote the boundaries of each substructure. The two red shadows denote the current sheets where exhausts are embedded. The ACE measurements are shifted by +24 min.

directed jets event, within a complex ICME at 1 AU. Observations show that the two reconnection events are component merging, quasi steady and fast reconnection, which are consistent with the previous results, and they are associated with two large-scale current sheets close to the centers of the sub flux ropes. Reconnections across these near-center current sheets may have a special consequence as discussed below.

2. Observations and Analysis

2.1. A Complex ICME on 26–27 November 2000

[6] Figure 1 displays a complex structure (between "A" and "B") during 26–27 November 2000 observed by ACE and Wind. This structure has been discussed in several papers. *Burlaga et al.* [2002] considered it as a part of a "complex ejecta" [*Burlaga et al.*, 2001] which were associated with several successive CMEs that interacted between the Sun and Earth. *Wang et al.* [2002] identified it to be a multiple magnetic cloud, which contained 4 subclouds bounded by five red dashed lines. However, *Cane and Richardson* [2003] did not relate it to any ICME when summarizing the ICMEs in the near-Earth solar wind during 1996–2002. Since a complex ICME could be related to successive CMEs as well as a single complicated non-MC-like ICME, we basically believe that it is a complex ICME detected here, based on the signatures of an apparent leading fast shock (marked by "S" in the "V_p" panel), enhancement of field strength (relative to the solar wind) and a large smooth rotation of field direction. The nonmonotonic decreasing speed and clear hierarchies of the magnetic field magnitude imply that this complex ICME is composed of several substructures. We roughly agree with that the complex ICME consists of four substructures with their boundaries marked by the red dashed lines in Figure 1, because the magnetic field strength, plasma speed, proton density and temperature consistently change at the edges of the substructures. However, each substructure is characterized by small-scale (~hours), not depressed proton density and high proton temperature besides the enhanced magnetic field strength and relative smooth rotation of magnetic field direction, which indicate the substructures forming the complex ICME may be small-scale flux ropes [*Moldwin et al.*, 1995, 2000] rather than individual MCs, according to the criteria for the definition of the MCs.

[7] From Figure 1, we can see that both ACE and Wind measurements show similar strong fluctuations, including discontinuities and local current sheets, throughout the

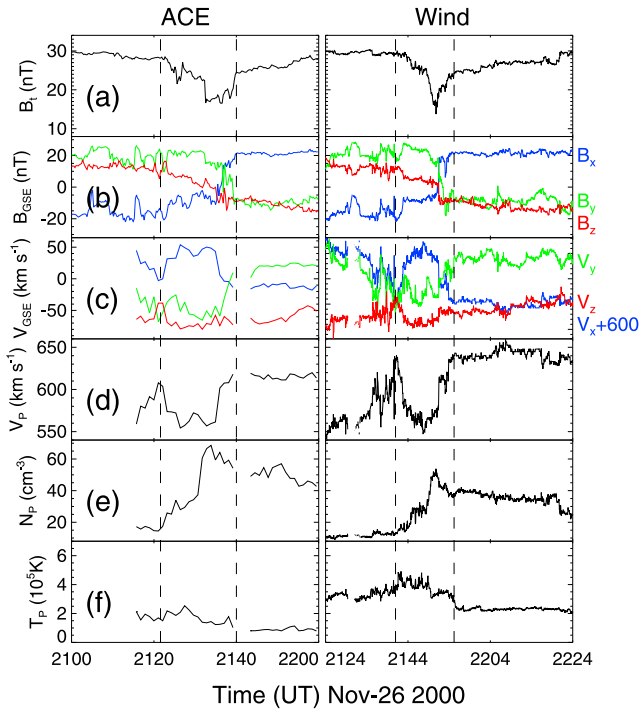

Figure 2. (a–f) (left) ACE 1 min (right) Wind 3 s: measurements in GSE of magnetic field strength and components, proton velocity components, density, and temperature from 2100 to 2200 UT (2124 to 2224 UT) on 26 November 2000. The vertical dashed lines denote the edges of the exhaust.

entire complex ICME. The red vertical shadows indicate the current sheets into which the exhausts are embedded. They are well inside the second and third flux rope, respectively. In the red shadows, we can find a drop in the field strength and corresponding abrupt changes in the magnetic azimuth and latitude angles as well as enhancements in plasma density and temperature and increase or decrease of the plasma speed (suggesting reconnection jets). Interestingly, during a short interval of about 4.5 h, i.e., from 26 November 2140 UT to 27 November 0210 UT, there are two X line exhaust events observed in association with large-scale current sheets close to the centers of the sub flux ropes.

2.2. Event 26 November 2000

[8] Figure 2 shows selected plasma and magnetic field data from ACE (left) and Wind (right) in GSE coordinates around the same bifurcated current sheet on 26 November 2000. At 2121–2140 UT, ACE first crossed the current sheet at [224.9, 35.1, −16.9] R_E GSE. Then, about 20 min later (2141–2154 UT), Wind spacecraft encountered the same current sheet at the location of [77.8, 92.6, −0.3] R_E GSE, downstream of ACE. We use the average bulk speed timing spacecraft traversal time to estimate the spatial width of the current sheet, which exceeds 6.8×10^5 km (~10000 ion inertial lengths).

[9] Figures 2a, 2d, and 2e exhibit a big drop (~50% at Wind) in the magnetic field strength and strong enhancements in proton density and temperature (relative to the ambient plasma). It should be pointed out that there is a big jump of a factor of 4 in proton density across the exhaust, indicating an asymmetric reconnection. Figures 2b and 2c show a pair of correlated and anticorrelated variations in magnetic field and velocity vector at the leading and trailing edges, respectively. The field shear across the current sheet is ~155° similar at both spacecraft, implying guide field reconnection. And the stronger positive enhancement in the x component of velocity indicates a largely sunward-directed exhaust here.

[10] To analyze the current sheets, we construct a LMN coordinate system where the N component is the normal to the current sheet, the M component is the X line orientation and L component is along the reconnection jets. We first perform a minimum variance analysis of magnetic field (MVAB) [*Sonnerup and Cahill*, 1967] to determine the normal to the current sheet, **N**. Afterward, we make use of the relation $\mathbf{M} = \mathbf{N} \times (\mathbf{B_A} - \mathbf{B_B})/|\mathbf{B_A} - \mathbf{B_B}|$, where $\mathbf{B_A}$ and $\mathbf{B_B}$ are the tangential magnetic field vectors on the two sides [*Sonnerup*, 1974] to calculate the X line orientation, **M**. And then $\mathbf{M} \times \mathbf{N}$ forms the L component.

[11] When performing the three steps above at ACE, we obtain a (**L**, **M**, **N**) of ([−0.72, 0.58, 0.38], [0.39, 0.79, −0.47], [−0.58, −0.19, −0.80]) GSE. The result from Wind is ([−0.70, 0.62, 0.35], [0.53, 0.78, −0.34], [−0.49, −0.05, −0.87]) GSE. Thus, the difference between the two results is only (3°, 11°, 10°) in L, M, and N components, respectively. This indicates that the current sheet is nearly one dimensional and quasi steady through ACE to Wind. In fact, the L component of magnetic field obtained directly from MVAB at Wind cannot reveal the bifurcated feature close to the leading edge of the exhaust, although the N direction turns out to be good. We then fix the N component and make a small adjustment on the L direction (also corresponding M direction) so that they can display the bifurcated nature of the exhaust and the L remains close to the maximum variance direction. The modified L and M directions are (−0.82, 0.37, 0.44) and (0.30, 0.93, −0.16) GSE. However, this adjustment will not affect the inference here.

[12] To identify the Alfvénic waves or rotational discontinuities bounding the exhaust, we perform a Walén test at Wind and ACE using the Walén relation [*Hudson*, 1970; *Paschmann et al.*, 1986]:

$$\mathbf{V}_{\text{predicted}} = \mathbf{V}_{\text{ref}} \pm (1 - \alpha_{\text{ref}})^{1/2} (\mu_0 \rho_{\text{ref}})^{-1/2} [(\rho_{\text{ref}}/\rho)\mathbf{B} - \mathbf{B}_{\text{ref}}] \quad (1)$$

Here, α is the pressure anisotropy factor and is defined as $\alpha \equiv (P_{\parallel} - P_{\perp})/\mu_0 |\mathbf{B}|^2$, where $P_{\parallel}$ and $P_{\perp}$ are the plasma pressures parallel and perpendicular to the magnetic field, respectively. The subscript "ref" denotes the reference time. In our calculations, α is assumed to be zero.

[13] Figure 3a presents the L, M and N components of the Wind magnetic field around the bifurcated current sheet: $\mathbf{B_N}$ is close to 0; $\mathbf{B_M}$ is strongly disturbed with a significant nonzero strength; and $\mathbf{B_L}$ changes significantly by ~−50.0 nT across the exhaust, suggesting that field rotation occurs almost entirely in the L direction. Figures 3b and 3c show the observed and predicted proton velocity magnitude and components by Walén test at Wind, respectively. In despite of strong fluctuations, Figure 3d shows an average shift of 17 km/s in the N component across the exhaust. Therefore, the speed of the reconnection inflow, V_{in}, is 8.5 km/s in the

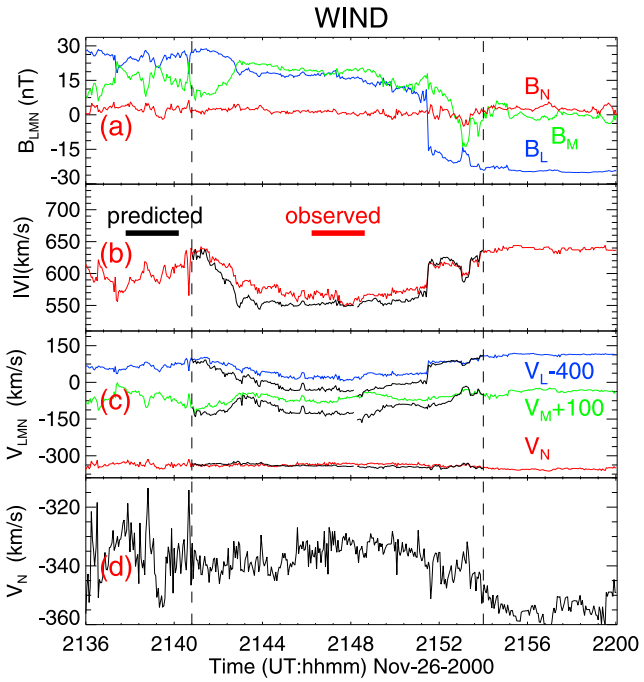

Figure 3. Event 26 November 2000 LMN analysis and Walén test from Wind data: (a) magnetic field components; (b) proton speed observed in red and predicted in black by Walén relation; (c) proton observed and predicted velocity components, the L component of the velocity has been shifted by −400 km/s; and (d) zoomed-in plot of the N component of proton velocity. The two vertical lines denote the edges of the exhaust (also the reference times in the Walén relation). The plus and minus are used in equation (1) for the leading and trailing edges, respectively.

frame of the current sheet. The dimensionless reconnection rate, V_{in}/V_A, is calculated to be about 5% in the upstream, where the Alfvén speed $V_A \simeq 180$ km/s, and it is larger in the downstream due to the larger proton density. Here, to avoid the problem of asymmetric reconnection rate, we simply believe that the dimensionless reconnection rate in this event is ≥5%, which is in the range of fast reconnection. Since the ACE observations are highly consistent with those from Wind, a similar result of LMN system and Walén test of low resolution from ACE is obtained (omitted here).

2.3. Event 27 November 2000

[14] About 4.5 h after the event on 26 November 2000, the two spacecraft detected an exhaust pair event in the third sub flux rope of the complex ICME. Figure 4 shows the selected plasma and field measurements of ACE (left) and Wind (right) around the bifurcated current sheet on 27 November 2000. The spatial width is about 2.5×10^5 km (~3000 ion inertial lengths).

[15] ACE first encountered the bifurcated current sheet between 0138–0145 UT and then during 0205–0208 UT, Wind spacecraft crossed the same current sheet. Figure 4a shows that there is a big drop (>50%) in the magnetic field strength. Figures 4e and 4f show that small enhancements in proton density and temperature occur within the exhaust at ACE and significant enhancements in the current sheet at Wind. Figure 4b shows consistent reversals of magnetic field components across the current sheet. Although there are large fluctuations in the three components of magnetic field, we can still verify a pair of correlated (anticorrelated) and anticorrelated (correlated) variations in **B** and **V** at the leading and trailing edges of the exhaust at ACE (Wind). The shear angles across the current sheet are 138° and 130° at ACE and Wind, respectively, much less than 180°, suggesting component field merging here. Figures 4c and 4d display the oppositely directed jets within the current sheet. The plasma jet detected at ACE has a maximum enhancement of [−51.88, −40.00, 22.70] km/s in the x, y and z components of velocity. By comparison, the obtained maximum enhancement at Wind is [64.59, 32.65, −24.38] km/s, thus, the angle between the two jets is 170°, nearly oppositely directed. Meanwhile, different plasma velocity and speed values are found between Wind and ACE measurements.

[16] We also construct a LMN system and perform a Walén test to derive the features of the current sheet and identify the Alfvénic waves bounding the exhausts. When performing the MVAB analysis at ACE, we find that the ratio between the intermediate and minimal variance directions is ≃1, i.e., 5.829 to 5.027, which means, in this case, no valid direction normal to the current sheet is obtained from MVAB, but the **L** remains a good vector tangential to the layer, and is calculated to be (0.70, 0.56, −0.44) GSE. While the L, M, and N directions of the Wind data from

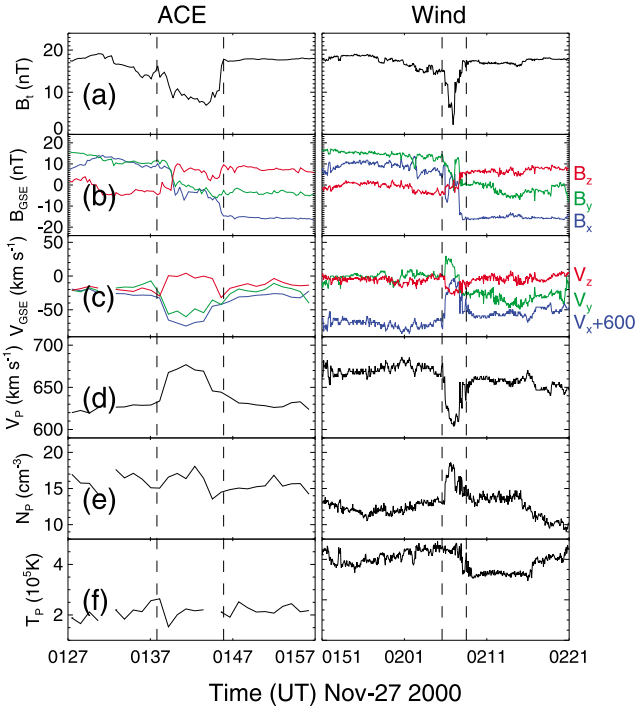

Figure 4. (a–f) (left) ACE 1 min (right) Wind 3 s: measurements in GSE of magnetic field strength and components, proton velocity components and magnitude, density, and temperature from 0127 to 0157 UT (0151 to 0221 UT) on 27 November 2000. The vertical dashed lines mark the edges of the exhaust.

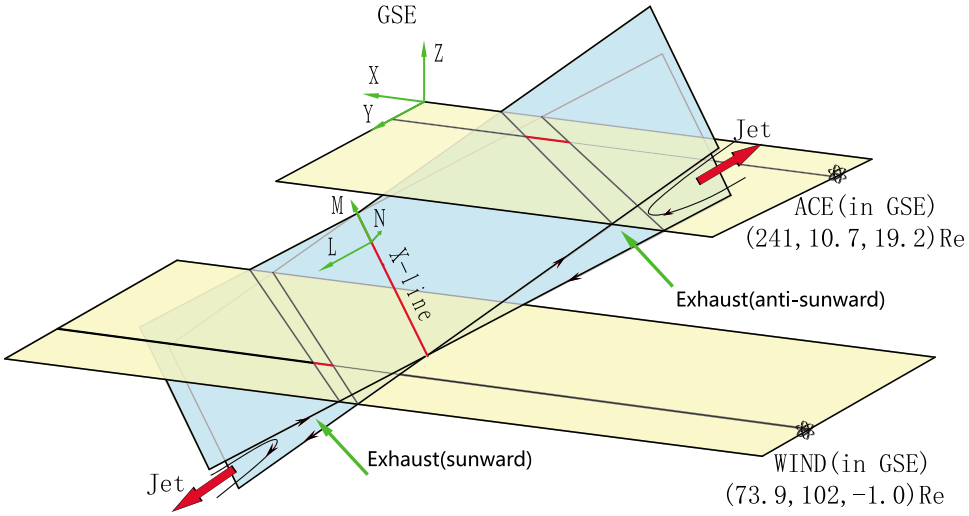

Figure 5. Schematic geometry of the bifurcated current sheet associated with the exhaust pair event and the relative location of the two spacecraft, the X line, and the oppositely directed exhaust.

MVAB are (0.83, 0.44, −0.34), (0.49, −0.87, 0.08) and (−0.26, −0.24, −0.94) GSE. The deviation between the two L components is only 7.2°, indicating that the current sheet is nearly flat. Figure 5 shows a schematic geometry of the current sheet into which the oppositely directed exhausts are embedded, based on the field and velocity profiles and locations of ACE and Wind. The traversal time of Wind is much shorter than that of ACE, and hence the Wind spacecraft is closer to the reconnection X line, which may be the reason why the enhancements in proton density and temperature are stronger at Wind (Figures 4e and 4f). The negative and positive enhancements in the x component of velocity (see Figures 4c and 4d) indicate that antisunward and sunward exhausts are observed by ACE and Wind, respectively.

[17] Figure 6a presents the L, M and N components of the magnetic field at Wind with a large rotation in the L direction and strong fluctuations. In this situation, the demonstration of the Alfvénic nature of the exhaust boundaries could not be well performed; besides, other reasons, such as the neglect of Alpha particles, could partly account for the discrepancy between observation and prediction. The dimensionless reconnection rate obtained from a shift of 11 km/s in $\mathbf{V_N}$ shown in Figure 6d is about 6% ($V_{in}/V_A \simeq 5.5/90 \simeq 6\%$), also suggesting fast reconnection.

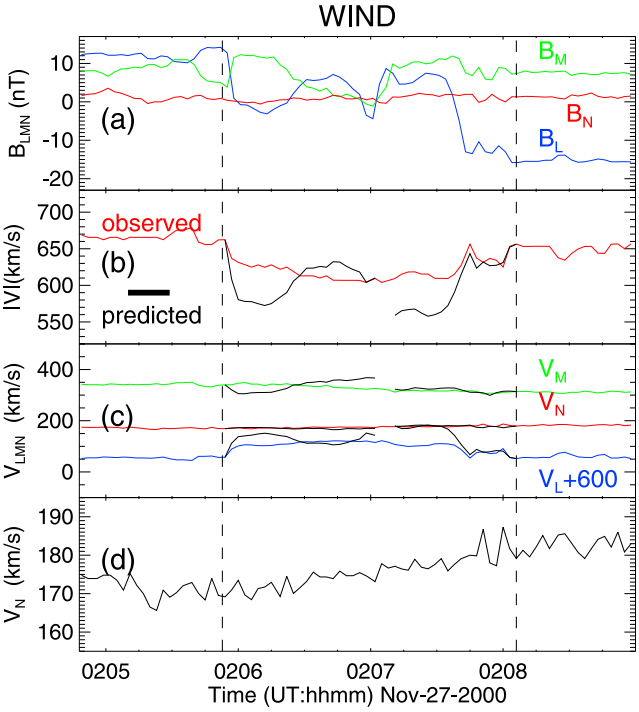

Figure 6. Event 27 November 2000 LMN analysis and Walén test from Wind data: (a) magnetic field components; (b) proton speed observed in red and predicted in black by Walén relation; (c) proton observed and predicted velocity components, the L component of the velocity has been shifted by +500 km/s; and (d) zoomed-in plot of the N component of proton velocity. The two vertical lines indicate the edges of the exhaust (also the reference times in the Walén relation). The plus and minus are used in equation (1) for the leading and trailing edges, respectively.

3. Discussion

[18] The two exhaust-associated bifurcated current sheets in our report are located close to the centers of sub flux ropes and separate the substructure into two parts of reversed magnetic field direction (Figure 1). These large-scale near-center current sheets are just of the same kind as reported by *Owens* [2009], who tried to use a kinematically distorted flux rope model [*Owens et al.*, 2006] to interpret the formation of these kinds of current sheets. Figure 7, adopted from *Owens* [2009], presents the schematic illustration of the near-center current sheets. Their basic char-

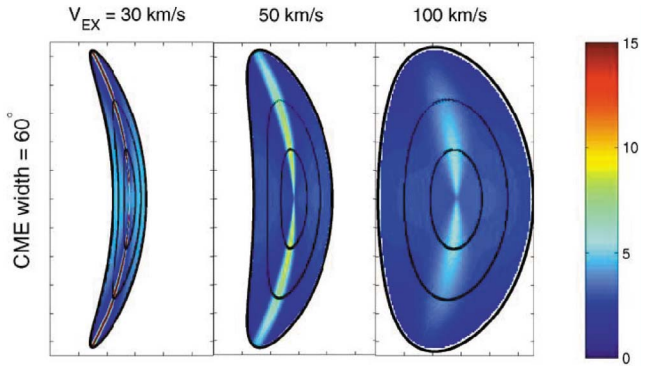

Figure 7. Adopted from *Owens* [2009], current density close to the center of a specific CME varies with the expansion speed; current sheets are most intense for small radial expansion speeds.

acteristics are large scale in spatial width, close to the center of the flux rope in geometry and separatrix of reversed magnetic field direction. *Owens* [2009] suggested that currents close to the centers of magnetic flux ropes increase in intensity and gradient as the angular width of the flux rope increases and the expansion speed decreases. When the angular width of a flux rope is fixed, the current density varies only with the expansion speed. Figure 7 shows that the current density becomes most intense for small radial expansion speed. In our report, the four flux ropes forming the complex ICME stay very close to each other so that it is hard for them to expand freely in the radial direction, especially for the central ones. In fact, we can verify this effect through the plasma speed profile in Figure 1. The trailing and leading edges of the second flux rope are moving roughly with the same speed, therefore, the second substructure is almost not expanding radially. The leading part of the third flux rope is going a little faster than the trailing part, thus, the third flux rope is mildly expanding radially. The relative lack of radial expansion could largely distort the central flux ropes and may lead to the formation of thin current sheets and reconnection near the centers of the distorted flux ropes according to *Owens* [2009].

[19] In addition, some local factors may also partly contribute to the formation of reconnection at these large-scale current sheets. In our first event, we see a strong enhancement by a factor of 4 in plasma density from upstream to downstream while the temperature and the field strength change a little (see Figure 2). Thus, the strong gradient of the total pressure of plasma (defined as $P_{total} = NK(T_i + T_e) + B^2/8\pi$, where N is the proton density, K is the Boltzmann constant, B is the field strength and T_i and T_e are the ion and electron temperatures, respectively) provides an external force to make the plasma merge. Figure 8 displays the total pressure of plasma (including the contribution from Alpha particles) around the exhaust. In the second event, different proton velocities between Wind and ACE observations are presented in Figure 4c. This may result from the instrumental effect. However, note that the deviation in the x component of the velocity between the two spacecraft is about 50 km/s, much larger than the average offset in Figure 1 (~20 km/s), and also larger than those in the y and z components, indicating that there may be shear flows almost along the x direction between the two spacecraft. And if shear flows perpendicular to the current sheet really exist between the oppositely directed exhausts, they could also contribute to the formation of reconnection. Figure 9 shows a sketch illustration of the simplest situation by assuming that the variation of the velocity normal to the current sheet is linear. So there must be a stationary point on each frozen-in field line, and the distance between any two stationary points will not change. If the initial distance between two field lines is d_0 (Figure 9a), then after a time interval of Δt, the distance between the same field lines will become $d = d_0 \sin\theta < d_0$ (Figure 9b) where $\theta = f(\Delta t)$ is the angle between the stationary point line and the field line. That means the current sheet will become thinner and thinner as time passes by until the frozen-in condition is broken.

4. Summary

[20] In this paper, we have identified two Petschek-like exhaust events within the interior of a complex ICME by ACE and Wind in detail. Observations show that both reconnection events are (1) guide field reconnection with shear angles much less than 180°, consistent with the result that almost all reconnection events in the solar wind are associated with strong guide fields [*Gosling et al.*, 2007c]; (2) fast reconnection with dimensionless rates of at least 5%, similar to the results of 3% [*Davis et al.*, 2006] and 3.3%

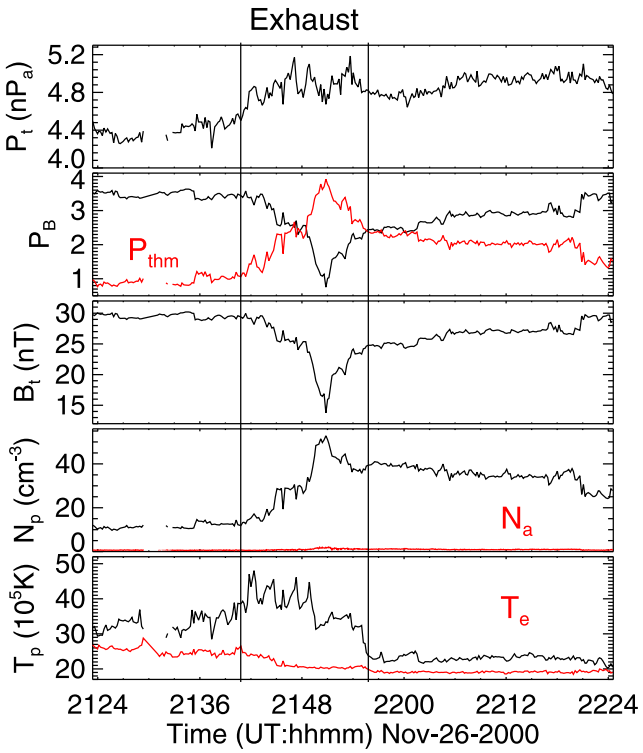

Figure 8. Plasma total pressure around the exhaust in event 26 November 2000. (top to bottom) Total pressure (P_t); magnetic pressure in black (P_B) and thermal pressure in red (P_{thm}); magnetic strength (B_t); proton density in black (N_p) and Alpha particles density in red (N_a); proton temperature in black (T_p) and electron temperature in red (T_e).

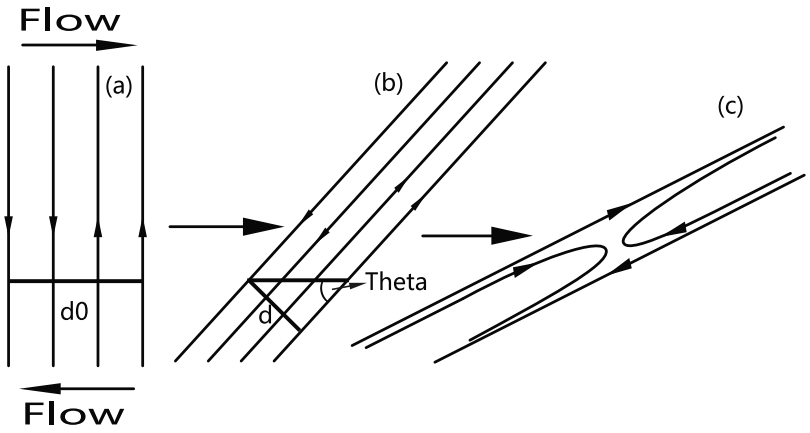

Figure 9. Sketch illustration of linear shear flows perpendicular to the current sheet. (a) The initial state: the line perpendicular to the current sheet connects two stationary points and its length, d_0, which is also the distance between two field lines, will not change. (b) After a time interval, the distance between the same field lines becomes $d = d_0 \sin\theta < d_0$, suggesting that the current sheet becomes thinner. (c) The thinning process will keep on until the frozen-in condition is broken.

[*Phan et al.*, 2006]; and (3) quasi steady over the scale of the traversal time from ACE to Wind in despite of intricate disturbance within the interior of the ICME, which is also consistent with the reports of the multiple spacecraft observations of the solar wind exhausts [*Davis et al.*, 2006; *Gosling et al.*, 2007a; *Phan et al.*, 2006, 2009].

[21] Figure 10 displays a sketch of the two spacecraft crossing the reconnection exhausts: Wind and ACE first detected a sunward-directed exhaust at the same side from the reconnection X line and then encountered an exhaust pair, i.e., a sunward exhaust at Wind and an antisunward exhaust at ACE. These exhausts are found to be associated with large-scale current sheets close to the centers of sub flux ropes. Exhausts within ICMEs, including some near-center cases, have been reported [*Gosling et al.*, 2005a, 2007b; *Gosling and Szabo*, 2008]. However, to the best of our knowledge, this paper is the first time to date to report reconnection exhausts related to current sheets of the three characteristics: large scale, close to the center and separatrix of reversed field direction. As pointed out by *Owens* [2009], reconnection at the centers of flux ropes may cause an interesting consequence. It can be easily seen from Figure 10 that the observed quasi-steady reconnections together with other possibly existing ones across the near-center current sheets would change the entire topology of the sub flux ropes and even fragment them into smaller ones. However, it can be only inferred by dual spacecraft observations. And multiple points detections of more spacecraft are required to confirm it.

[22] **Acknowledgments.** We thank the principal investigators, R. P. Lin, R. Lepping, D. J. McComas, N. Ness, and CDAWeb for use of the data of Wind/3DP and Wind/MFI and ACE/SWEPAM and ACE/MAG in this paper. We also thank the reviewers for their helpful comments. This work is jointly supported by the National Natural Science Foundation of China (40890162, 40921063, 40904049, and 41031066) and the Specialized Research Fund for State Key Laboratories.

[23] Philippa Browning thanks John Gosling and another reviewer for their assistance in evaluating this paper.

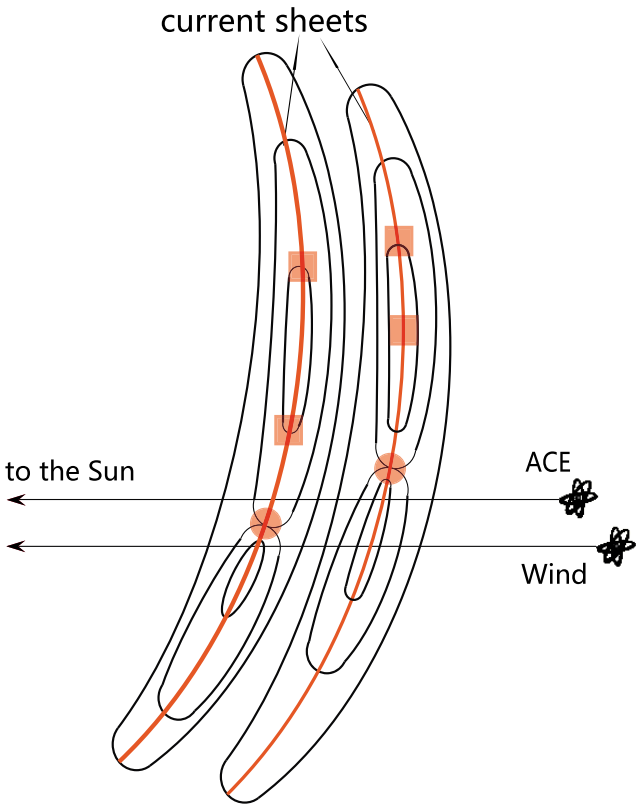

Figure 10. A sketch of the ACE and Wind spacecraft crossing the reconnection exhausts associated with two distorted flux ropes within a complex ICME during 26–27 November 2000. The red circles mark the reconnection regions detected, and the red squares indicate the possibly existing reconnection sites. These quasi-steady reconnections may fragment single flux rope into smaller ones.

References

Burlaga, L., E. Sittler, F. Mariani, and R. Schwenn (1981), Magnetic loop behind an interplanetary shock: Voyager, Helios, and IMP 8 observations, *J. Geophys. Res.*, *86*, 6673–6684.

Burlaga, L., R. Skoug, C. Smith, D. Webb, T. Zurbuchen, and A. Reinard (2001), Fast ejecta during the ascending phase of solar cycle 23: ACE observations, 1998–1999, *J. Geophys. Res.*, *106*, 20,957–20,977.

Burlaga, L. F., S. P. Plunkett, and O. C. St. Cyr (2002), Successive CMEs and complex ejecta, *J. Geophys. Res.*, *107*(A10), 1266, doi:10.1029/2001JA000255.

Cane, H. V., and I. G. Richardson (2003), Interplanetary coronal mass ejections in the near-Earth solar wind during 1996–2002, *J. Geophys. Res.*, *108*(A4), 1156, doi:10.1029/2002JA009817.

Davis, M. S., T. D. Phan, J. T. Gosling, and R. M. Skoug (2006), Detection of oppositely directed reconnection jets in a solar wind current sheet, *Geophys. Res. Lett.*, *33*, L19102, doi:10.1029/2006GL026735.

Fainberg, J., V. A. Osherovich, R. G. Stone, R. J. MacDowall, and A. Balogh (1996), Ulysses observations of electron and proton components in a magnetic cloud and related wave activity, paper presented at 8th international solar wind conference, p. 554, Am. Inst. Phys., Woodbury, N. Y.

Gosling, J. T. (2007), Observations of magnetic reconnection in the turbulent high-speed solar wind, *Astrophys. J.*, *671*, L73–L76, doi:10.1086/524842.

Gosling, J. T., and A. Szabo (2008), Bifurcated current sheets produced by magnetic reconnection in the solar wind, *J. Geophys. Res.*, *113*, A10103, doi:10.1029/2008JA013473.

Gosling, J. T., R. M. Skoug, D. K. Haggerty, and D. J. McComas (2005a), Absence of energetic particle effects associated with magnetic reconnection exhausts in the solar wind, *Geophys. Res. Lett.*, *32*, L14113, doi:10.1029/2005GL023357.

Gosling, J. T., R. M. Skoug, D. J. McComas, and C. W. Smith (2005b), Direct evidence for magnetic reconnection in the solar wind near 1 AU, *J. Geophys. Res.*, *110*, A01107, doi:10.1029/2004JA010809.

Gosling, J. T., S. Eriksson, L. M. Blush, T. D. Phan, J. G. Luhmann, D. J. McComas, R. M. Skoug, M. H. Acuna, C. T. Russell, and K. D. Simunac (2007a), Five spacecraft observations of oppositely directed exhaust jets from a magnetic reconnection X line extending $> 4.26 \times 10^6$ km in the solar wind at 1 AU, *Geophys. Res. Lett.*, *34*, L20108, doi:10.1029/2007GL031492.

Gosling, J. T., S. Eriksson, D. J. McComas, T. D. Phan, and R. M. Skoug (2007b), Multiple magnetic reconnection sites associated with a coronal mass ejection in the solar wind, *J. Geophys. Res.*, *112*, A08106, doi:10.1029/2007JA012418.

Gosling, J. T., T. D. Phan, R. P. Lin, and A. Szabo (2007c), Prevalence of magnetic reconnection at small field shear angles in the solar wind, *Geophys. Res. Lett.*, *34*, L15110, doi:10.1029/2007GL030706.

Hudson, P. D. (1970), Discontinuities in an anisotropic plasma and their identification in the solar wind, *Planet. Space Sci.*, *18*, 1611–1622.

Lugaz, N., W. B. Manchester IV, and T. I. Gombosi (2005), Numerical simulation of the interaction of two coronal mass ejections from Sun to Earth, *Astrophys. J.*, *634*, 651.

Moldwin, M. B., J. L. Phillips, J. T. Gosling, E. E. Scime, D. J. McComas, S. J. Bame, A. Balogh, and R. J. Forsyth (1995), Ulysses observation of a noncoronal mass ejection flux rope: Evidence of interplanetary magnetic reconnection, *J. Geophys. Res.*, *100*, 19,903–19,910, doi:10.1029/95JA01123.

Moldwin, M. B., S. Ford, R. Lepping, J. Slavin, and A. Szabo (2000), Small-scale magnetic flux ropes in the solar wind, *Geophys. Res. Lett.*, *27*, 57–60, doi:10.1029/1999GL010724.

Mozer, F. S., S. D. Bale, and T. D. Phan (2002), Evidence of diffusion regions at a subsolar magnetopause crossing, *Phys. Rev. Lett.*, *89*, 015002, doi:10.1103/PhysRevLett.89.015002.

Øieroset, M., T. D. Phan, M. Fujimoto, R. P. Lin, and R. P. Lepping (2001), In situ detection of collisionless reconnection in the Earth's magnetotail, *Nature*, *412*, 414–417.

Owens, M. J. (2009), The formation of large-scale current sheets within magnetic clouds, *Solar Phys.*, *260*, 207–217.

Owens, M. J., V. G. Merkin, and P. Riley (2006), A kinematically distorted flux rope model for magnetic clouds, *J. Geophys. Res.*, *111*, A03104, doi:10.1029/2005JA011460.

Paschmann, G., I. Papamastorakis, W. Baumjohann, N. Sckopke, C. W. Carlson, B. U. Ö. Sonnerup, and H. Lühr (1986), The magnetopause for large magnetic shear: AMPTE/IRM observations, *J. Geophys. Res.*, *91*, 11,099–11,115.

Petschek, H. E. (1964), Magnetic annihilation, in *AAS-NASA Symposium on the Physics of Solar Flares*, edited by W. N. Hess, *NASA Spec. Publ., SP-50*, 425.

Phan, T. D., et al. (2006), A magnetic reconnection X line extending more than 390 Earth radii in the solar wind, *Nature*, *439*, 175–178.

Phan, T. D., J. T. Gosling, and M. S. Davis (2009), Prevalence of extended reconnection X lines in the solar wind at 1 AU, *Geophys. Res. Lett.*, *36*, L09108, doi:10.1029/2009GL037713.

Schmidt, J. M., and P. J. Cargill (2003), Magnetic reconnection between a magnetic cloud and the solar wind magnetic field, *J. Geophys. Res.*, *108*(A1), 1023, doi:10.1029/2002JA009325.

Sonnerup, B. U. Ö. (1974), Magnetopause reconnection rate, *J. Geophys. Res.*, *79*, 1546–1549.

Sonnerup, B. U. Ö., and L. J. Cahill Jr. (1967), Magnetopause structure and attitude from Explorer 12 observations, *J. Geophys. Res.*, *72*, 171–183.

Vaivads, A., Y. Khotyaintsev, M. André, A. Retinò, S. C. Buchert, B. N. Rogers, P. Décréau, G. Paschmann, and T. D. Phan (2004), Structure of the magnetic reconnection diffusion region from four-spacecraft observations, *Phys. Rev. Lett.*, *93*, 105001, doi:10.1103/PhysRevLett.93.105001.

Wang, Y. M., S. Wang, and P. Z. Ye (2002), Multiple magnetic clouds in interplanetary space, *Sol. Phys.*, *211*, 333–344.

Zurbuchen, T. H., and I. G. Richardson (2006), In-situ solar wind and magnetic field signatures of interplanetary coronal mass ejections, *Space Sci. Rev.*, *123*, 31–43, doi:10.1007/s11214-006-9010-4.

X. Feng, F. Wei, and X. Xu, SIGMA Weather Group, State Key Laboratory of Space Weather, Center for Space Science and Applied Research, Chinese Academy of Sciences, PO Box 8701, Beijing 100190, China. (fengx@spaceweather.ac.cn; fswei@spaceweather.ac.cn; xjxu@spaceweather.ac.cn)